(11) J. P. Collman, J. L. Hoard, N. Kim, G. Land, and C. A. Read, *J. Am. Chem. Soc.*, **97**, 2676 (1975).
(12) J. P. Collman, J. I. Brauman, T. R. Halbert, and K. S. Suslick, *Proc. Natl. Acad. Sci. U.S.A.*, **73**, 3333 (1976).
(13) C. H. Barlow, J. C. Maxwell, W. J. Wallace, and W. S. Caughey, *Biochem. Biophys. Res. Commun.*, **58**, 166 (1973).
(14) L. Pauling, *Nature (London)*, **203**, 182 (1964).
(15) J. B. R. Dunn, D. F. Shriver, and I. M. Klotz, *Proc. Natl. Acad. Sci. U.S.A.*, **70**, 2582 (1973).
(16) T. C. Strekas and T. G. Spiro, *Inorg. Chem.*, **14**, 421 (1975).

Electronic Structure of $M_4(CO)_{12}H_n$ and $M_4Cp_4H_n$ Complexes

Roald Hoffmann,*[1a] Birgitte E. R. Schilling,[1a] Robert Bau,[1b] Herbert D. Kaesz,[1c] and D. Michael P. Mingos[1d]

Contribution from the Department of Chemistry, Cornell University, Ithaca, New York 14853, Department of Chemistry, University of Southern California, Los Angeles, California 90007, Department of Chemistry, University of California, Los Angeles, California 90024, and Inorganic Chemistry Laboratory, University of Oxford, Oxford, England OX1 3QR. *Received August 26, 1977*

Abstract: The electronic structure of tetranuclear hydrido clusters $M_4(CO)_{12}H_n$ and $M_4Cp_4H_n$, n = 3, 4, 6, is analyzed with the aid of symmetry arguments and molecular orbital calculations. The orbitals of the clusters are derived by protonating $M_4(CO)_{12}$ and M_4Cp_4 tetrahedra. The important levels of these are the inward and surface-like higher occupied orbitals of $a_1 + e + t_2$ symmetry (plus a low-lying unfilled t_1 orbital occupied by three electrons in the electron-rich $Ni_4Cp_4H_3$ cluster). The electron distribution in the surface orbitals e and t_2 is studied as a function of staggered or eclipsed carbonyl orientation and along the edges or faces of the tetrahedron. The results of this study provide an understanding of the variable location of hydrogens in these clusters.

This paper is concerned with the electronic structure of tetranuclear hydrido clusters of the type $M_4(CO)_{12}H_n$ and $M_4Cp_4H_n$, Cp = cyclopentadienyl, M = a transition metal, and n = 3, 4, or 6. The well-characterized molecules in this series share the basic feature of a near-tetrahedral disposition of the metal centers, but then diverge to exhibit staggered, **1**, or eclipsed, **2**, orientations of the carbonyl groups (relative to

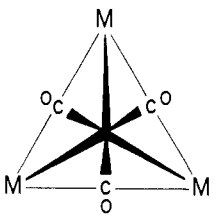

1

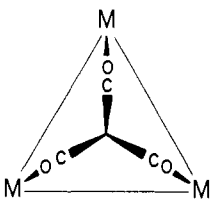

2

the metal–metal edges), and edge- or face-bridging hydrogens. They may also possess varying spin states and propensities to hydrogen mobility. This choice of geometrical and electronic structure is of interest to us.

Let us review what is known about these molecules, making reference only to well-established geometrical facts, and keeping in mind the problems associated with accurately locating hydride positions in X-ray crystallographic structures. $Re_4(CO)_{12}H_4$[2a] has four face-bridging hydrides and eclipsed carbonyl groups.[2b] $Re_4(CO)_{12}H_6^{2-}$ has staggered carbonyls, and the hydrides are presumably edge-bridging,[3] though this has not been definitely established. $Ru_4(CO)_{12}H_4$ has been synthesized[4] and a D_{2d} geometry with edge-bridging hydrides (**3**) established through X-ray diffraction.[5] In addition crystallographic studies on the derivatives $Ru_4(CO)_{11}H_4P(OCH_3)_3$,[2b] $Ru_4(CO)_{10}H_4(PPh_3)_2$,[5] and $Ru_4(CO)_{10}H_4$(diphos)[6] all show staggered carbonyls and four edge-bridging hydrides, though the disposition of the edges bearing hydrides differs: $Ru_4(CO)_{12}H_4$, $Ru_4(CO)_{11}H_4P(OCH_3)_3$, and $Ru_4(CO)_{10}H_4(PPh_3)_2$ have configuration **3**,[5] while

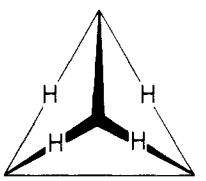

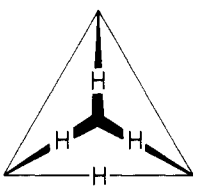

3 4

$Ru_4(CO)_{10}H_4$(diphos) has configuration **4**. Hydride motions are complex and interesting in these Ru compounds.[4,6]

In the cyclopentadienyl complexes the question of eclipsing or staggering is a moot one, since the barrier of rotation of a fivefold rotor such as an η^5-cyclopentadienyl ring against the pseudo-threefold rotor presented to it by a metal vertex of the tetrahedron is expected to be small. $Co_4Cp_4H_4$ is known[7] and face-bridging hydrogens have been inferred from the crystal structure.[8] $Ni_4Cp_4H_3$ has also been synthesized[9] and has been studied by X-ray[10] and neutron[11] diffraction. Both methods concur in showing three face-bridging hydrogens. This compound is especially interesting because, in contrast to all molecules mentioned above, it is paramagnetic, with three unpaired electrons.[9]

The Orbitals of $M_4(CO)_{12}$

The natural construction of the electronic structure of the molecules is from the orbitals of tetrahedral $M_4(CO)_{12}$, **5**, or M_4Cp_4, **6**, interacting with three to six hydrogen atoms. In the real molecule the hydrogens may exhibit extremes of hydridic or protonic character, or some behavior in between—this will not affect our analysis which finds it convenient to begin with the formalism of an "electron-precise" or "saturated" cluster $Ir_4(CO)_{12}$ or Ni_4Cp_4 and to think of protonating that cluster or removing some electrons from it.

The electronic structure of these saturated clusters is well understood.[12-15] The $Ir(CO)_3$ and NiCp fragments are isolo-

0002-7863/78/1500-6088$01.00/0

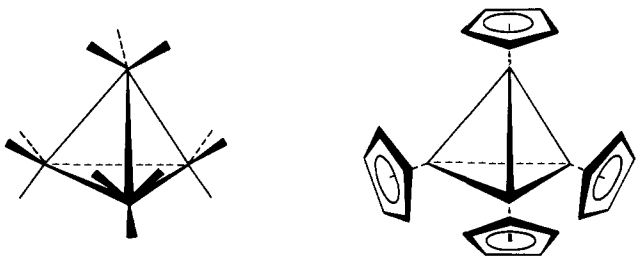

5 6

bal[16] with each other, and with CH or BH^-. The transition metal fragments are characterized by six frontier orbitals, as shown in **7**. Three are low lying, the descendants of the octa-

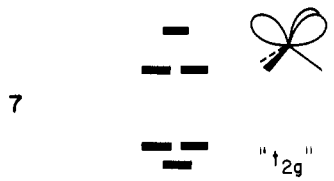

7

hedral t_{2g} set. These low-lying orbitals are primarily d in character and interact little with neighboring metal atoms. Whatever directionality they have comes to the fore in the $M(CO)_3$ fragment where they are so disposed in space that they eclipse the three carbonyls.[17]

More important are the three higher orbitals. These have significant admixtures of metal s and p, making for greater overlaps with neighboring metal atoms and bridging ligands.[18] The three delocalized orbitals, $a_1 + e$, are the equivalent of three localized hybrids completing an octahedron around the metal atom. This quasi-octahedral directionality is pronounced in $M(CO)_3$ and will figure importantly in setting the orientation of the carbonyls in the cluster as staggered or eclipsed. In MCp the directionality is suppressed.[16,17]

In $Ir_4(CO)_{12}$ and Ni_4Cp_4 each metal carries nine d electrons. Six of these are lone-pair-like, in the lower "t_{2g}" set, three in the upper set of valence orbitals. One has one electron per hybrid, with the consequence that localized electron pairing can occur along the edges of the tetrahedron. This is the reason for calling these clusters saturated and analogous to tetrahedrane (or P_4).[12-15]

The 12 orbitals formed by the four sets of three high-lying hybrids at each $M(CO)_3$ or MCp fragment transform as $a_1 + e + t_1 + 2t_2$. These may be partitioned further in two ways. The a_1 combination of the individual fragment points inward, toward the center of the cluster, while the e combinations are more surface-like, tangential, peripheral. The inward orbitals generate $a_1 + t_2$, the surface set $e + t_1 + t_2$.[19] The presence of t_2 in both sets is a sign that the inward-surface partitioning is not clean. The other partitioning focuses on the localized bonding model of six electron pairs along tetrahedral edges.[12-15,19-22] It leads to six bonding molecular orbitals (MOs) of $a_1 + e + t_2$ symmetry and six antibonding combinations, $t_1 + t_2$.

The detailed ordering of the valence orbitals of the saturated cluster was obtained from a calculation on a model $Fe_4(CO)_{12}^{4-}$, using the extended Hückel method, with parameters listed in the Appendix. Since the hydrido clusters show both staggered and eclipsed carbonyl orientations, **1** and **2**, the calculation was done for both cases. The frontier orbitals are shown in Figure 1. In each geometry the $a_1 + e + t_2$ occupied set of cluster orbitals is at high energy, fairly well separated from other orbitals. This supports the general picture of bonding in these clusters that has been assembled previously[12-17] and gives us some confidence that the primary effects of protonation may be gleaned by focusing on these orbitals alone.

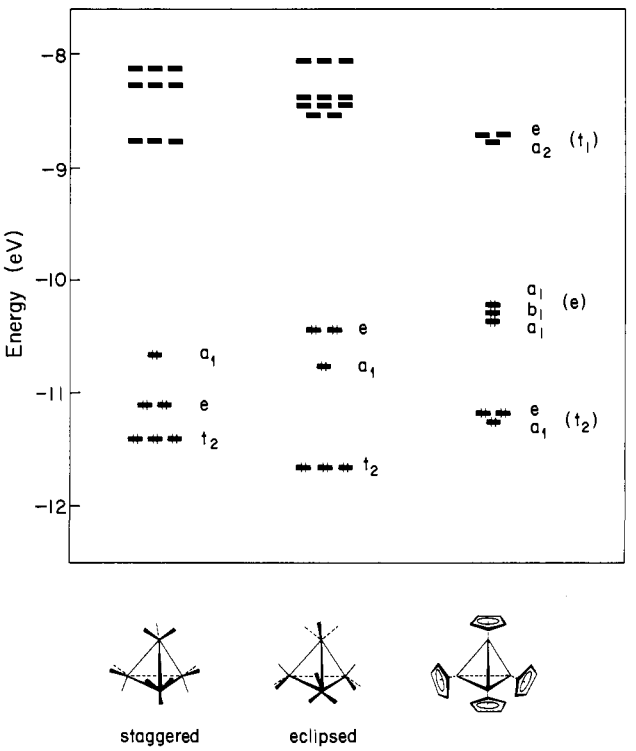

Figure 1. Frontier orbitals of $Fe_4(CO)_{12}^{4-}$ with staggered and eclipsed carbonyl groups, and $Fe_4Cp_4^{8-}$.

The staggered geometry of the saturated cluster is preferred to the eclipsed one by 2.0 eV in our calculations. Most, but not all, of that bias is in the $a_1 + e + t_2$ set of higher occupied MOs. The a_1 orbital is oriented inward and is not sensitive to carbonyl orientation. The e orbital is considerably lower in energy in the staggered geometry, and the t_2 somewhat higher in the same conformation. Since these orbitals are crucial in our further discussion of protonation, we pause here to explain these energy trends.

Let us begin with a basis set of three hybrid orbitals per metal center in the staggered geometry, **8**, and the eclipsed, **9**. One line of reasoning is to simply say that **8** is better set up

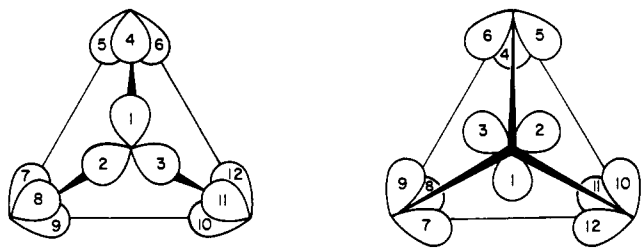

8 9

for edge bonding, while **9** is prepared for face bonding. Edge bonding implies six bonding orbitals, $a_1 + e + t_2$, as mentioned above. Analyzed in a primitive manner, face bonding means that from the three orbitals pointing into a face in **9** one forms three MOs, locally of a + e symmetry. Of these only one is bonding, the in-phase a combination. Combining four such faces, one will get in the full tetrahedron really only four bonding combinations, of $a_1 + t_2$ symmetry. In the eclipsed or face-bonded structure the e combination is descended from an antibonding orbital, and so lies at high energy. Conversely, the t_2 orbital is more bonding in the eclipsed structure than in the staggered one.

Another line of reasoning begins with the construction of the proper symmetry-adapted linear combinations for the two

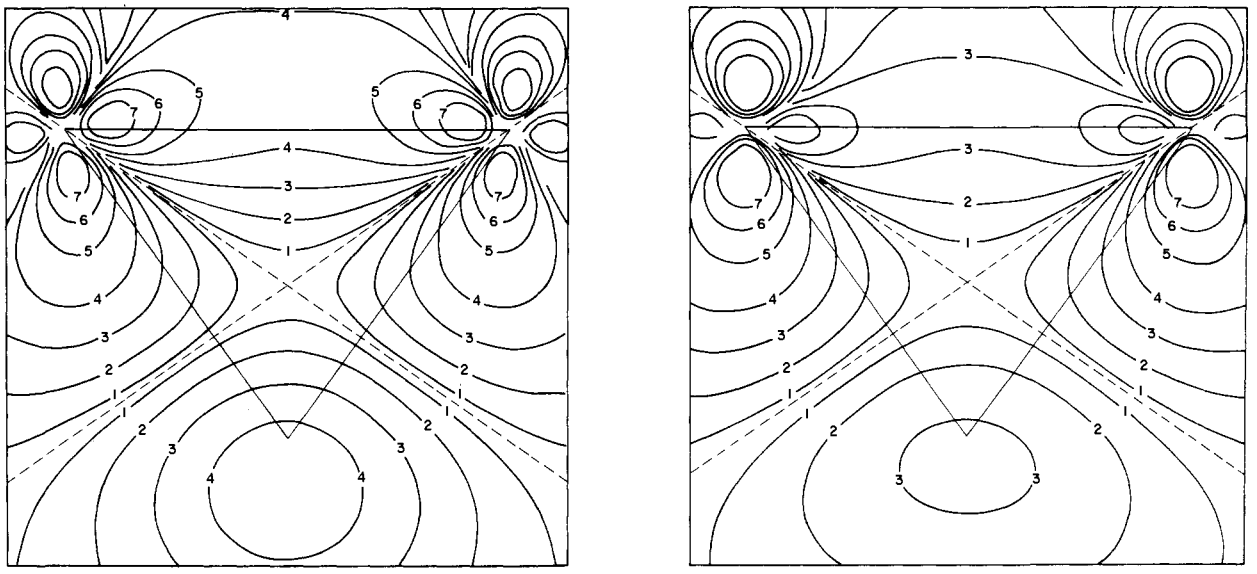

Figure 2. Density plots of the metal part of the e set of $Fe_4(CO)_{12}$. The wave function has been squared and summed over the two degenerate levels. The occupation is thus formally one electron per level. The plots are in one of the mirror planes of the molecule, with the horizontal line representing a metal-metal bond. The values shown on the contours indicate the variation in Ψ^2, and the relationship to the actual values of the contours is as follows: 1 = 0.000 05, 2 = 0.0005, 3 = 0.002, 4 = 0.005, 5 = 0.0125, 6 = 0.025, 7 = 0.05. The dashed lines show nodes.

geometries. Given the degeneracy, there is no unique way to do this for the e and t_2 wave functions. One choice is given below, unnormalized.

$$e \begin{cases} 2(\varphi_1 + \varphi_4) + 2(\varphi_9 + \varphi_{10}) - (\varphi_2 + \varphi_8) - (\varphi_3 + \varphi_{11}) \\ \quad - (\varphi_5 + \varphi_7) - (\varphi_6 + \varphi_{12}) \\ (\varphi_2 + \varphi_8) - (\varphi_3 + \varphi_{11}) + (\varphi_5 + \varphi_7) - (\varphi_6 + \varphi_{12}) \end{cases} \quad (1)$$

$$t_2 \begin{cases} (\varphi_1 + \varphi_4) - (\varphi_9 + \varphi_{10}) \\ (\varphi_2 + \varphi_8) - (\varphi_6 + \varphi_{12}) \\ (\varphi_3 + \varphi_{11}) - (\varphi_5 + \varphi_7) \end{cases} \quad (2)$$

φ_i is a hybrid orbital as numbered in **8** or **9.** The orbitals are grouped to emphasize bonding pairs in the staggered conformation.

The tetrahedral symmetry imposes certain constraints on the electron density of various orbitals. Thus the t_2 orbital must have zero density at the center of the tetrahedron and the e orbital vanishes everywhere along the four threefold axes. The latter condition implies zero electron density in the tetrahedral face centers. Whatever bonding characteristics the e orbital has are concentrated along the edges. One of the e combinations in eq 1 is shown schematically in **10** and **11.** The point that

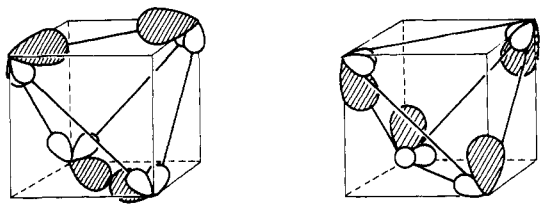

10 **11**

emerges is that edge bonding in the e orbital is significantly better in **10,** the staggered conformation, than in **11.** This is reinforced by Figure 2, an actual contour plot of the total electron density in the e orbital in one mirror plane of the tetrahedron.

The t_2 orbital has electron density over the edges and face centers. One of its components is shown in **12** and **13.** It is

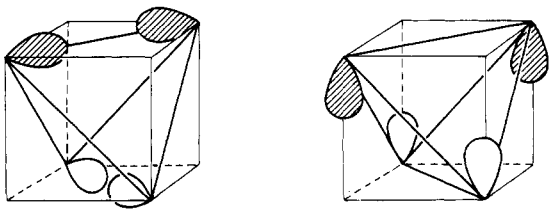

12 **13**

clearly more edge concentrated in **12,** face-like in **13.** The differential is less than it might seem from **12** and **13,** owing to the admixture of the higher t_2 set. Contour diagrams of the total electron density in the t_2 orbital for both the staggered conformation, somewhat bovine, and the eclipsed form, perhaps more porcine (or tigrine to one referee) in appearance, are presented in Figure 3. The basic point persists, namely, that t_2 is more bonding along the edges in the staggered geometry, more bonding along the faces in the eclipsed conformation. The face bonding turns out to be somewhat more important as far as the orbital energy is concerned.

To summarize, the e orbital is at higher energy in the eclipsed geometry, the t_2 at somewhat lower energy in the same geometry. As Figure 1 shows, the e orbital trend dominates. The staggered geometry is also favored by some lower orbital interactions. These are linear combinations of the set of three descended from the t_{2g} orbital of the octahedron, the bottom three orbitals in **7.** These orbitals are filled, so that interactions between them are repulsive. They also possess some directional character, though not as much as the upper set of three, and point to directions that complete a trigonal prism with the three carbonyls.[17] This is shown schematically in **14.** Four-electron destabilizations from these orbitals, while not large, are greater in the eclipsed geometry.

We have not discussed in any detail the M_4Cp_4 orbitals, though these are also shown in Figure 1. The fivefold axis of

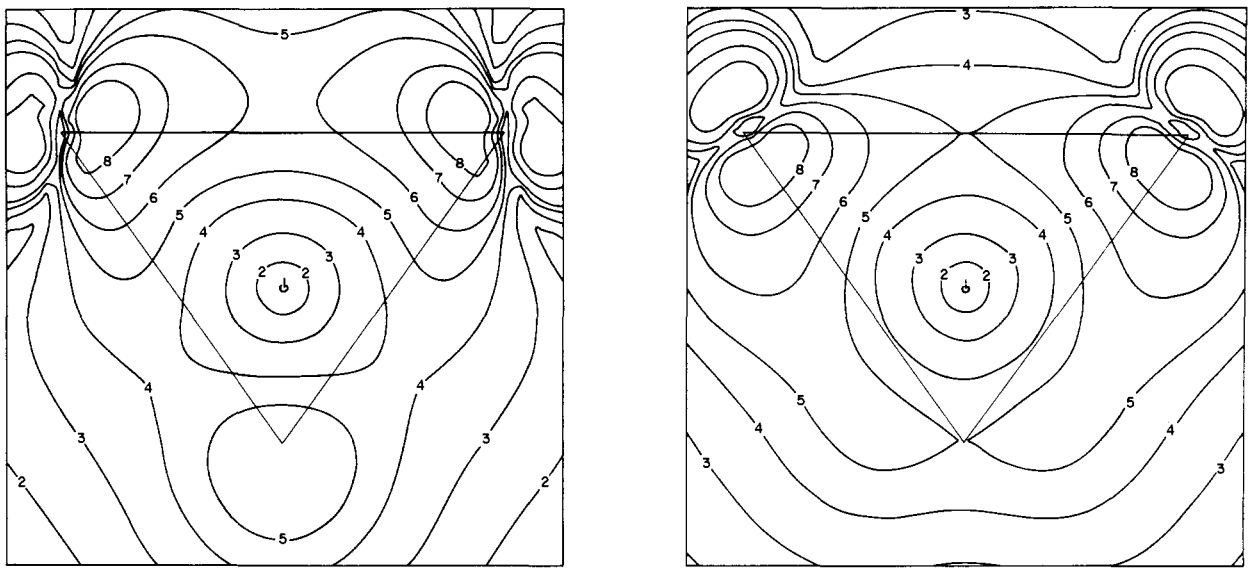

Figure 3. Density plots of the metal part of the t_2 set of $Fe_4(CO)_{12}$. The wave function has been squared and summed over the three degenerate levels. The occupation is thus formally one electron per level. The plots are in one of the mirror planes of the molecule, with the horizontal line representing a metal-metal bond. The values shown on the contours indicate the variation in Ψ^2, and the relationship to the actual values of the contours is as follows: 1 = 0.000 05, 2 = 0.0005, 3 = 0.002, 4 = 0.005, 5 = 0.008, 6 = 0.0125, 7 = 0.025, 8 = 0.05.

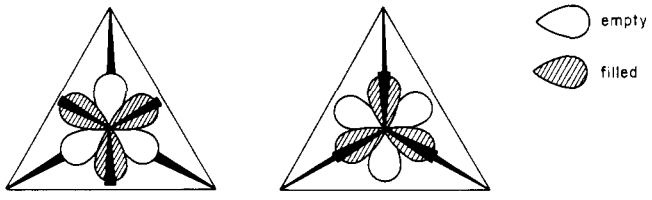

14

the Cp group is incommensurate with the threefold axis of the tetrahedron, so that the actual symmetry of any M_4Cp_4 geometry is lower than T_d. Of course the pseudotetrahedral nature of the complex is retained, so that splittings of the e and t_2 level as shown in Figure 1 are small. The basic pattern of high-lying $a_1 + e + t_2$ is preserved. The position of the "e" level in M_4Cp_4 is intermediate between the two $M(CO)_3$ cases discussed above, just about at the same energy as the a_1 level.

Construction of the Hydride Complexes

As we approach a number of protons to the edges or faces of $M_4(CO)_{12}$ or M_4Cp_4, the extent of interaction will be governed by the usual perturbation theoretic expression:

$$\Delta E = \frac{|H_{ij}|^2}{E_i - E_j} \qquad (3)$$

We will have to watch carefully the electron count to determine if the net interactions are stabilizing two-electron or destabilizing four-electron ones. But in either case the most important factor will be the overlap of an incoming proton with the framework orbitals of the tetrahedron. That overlap depends on the electron density and the arguments of the previous section may be summarized qualitatively in Table I. The inward pointing a_1 orbital has been omitted because it provides no differentiation between the various sites.

Six protons coming in along the edges, each bearing a 1s orbital, transform as $a_1 + e + t_2$. They interact beautifully with the high-lying MOs of a saturated cluster. Carbonyl staggering is preferred. The compound that we calculated is $Fe_4(CO)_{12}H_6^{2+}$, a model for the known isoelectronic species $Re_4(CO)_{12}H_6^{2-}$.[3]

Table I. Interactions of Tetrahedral Framework Orbitals with a Probe Hydrogen

	face	edge
e	0	staggered > eclipsed
t_2	eclipsed > staggered	staggered > eclipsed

Four protons coming in on face centers transform as $a_1 + t_2$. In $Fe_4(CO)_{12}H_4$ they would add a factor favoring the eclipsed carbonyl orientation, but that would be superimposed on the natural tendency for staggering. With four electrons less the e orbital which is unaffected by face protonation would be vacated. This is the orbital largely responsible for the staggered conformation of the saturated cluster $[Fe_4(CO)_{12}]^{4-}$ or $Ir_4(CO)_{12}$], so that in the electron-deficient system, e.g., $Re_4(CO)_{12}H_4$, there should be no ambiguity about eclipsing being preferred.

There are of course alternative edge-protonation patterns to be considered, of the type illustrated in **3** and **4** and found in various substituted Ru_4 clusters. If we retain 12 carbonyl groups, the protonated geometry analogous to **3** has D_{2d} symmetry, while that similar to **4** is reduced to a single mirror plane. We have analyzed only the D_{2d} structure in detail.

In D_{2d} four edge-bridging protons transform as $a_1 + b_1 + e$. The t_2 level reduces to $e + b_2$ and e to $a_1 + b_1$. Thus nearly all levels of the cluster are affected. It is clear that staggering of the carbonyls should be even better in the protonated cluster.

This is about as far as a qualitative analysis based on symmetry arguments can be pushed. The important question not answered is whether face protonation is better than edge protonation for four hydrogens. This involves a weighing of various interactions, and we resorted to a detailed calculation. Table II summarizes the results, the energies in each case referred to an arbitrary energy zero for the most stable calculated geometry.

First note that the computed energies support the qualitative

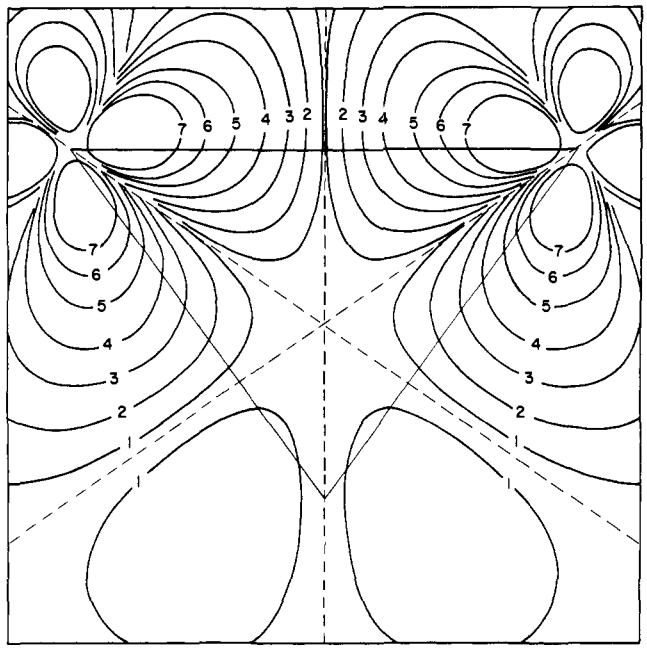

Fe_4Cp_4 "t_1"

Figure 4. A density plot of the metal part of the "t_1" orbital of Fe_4Cp_4. As before, the wave function has been squared and the formal occupation is one electron per level. The plot is in one mirror plane of the molecule with the metal-metal bond horizontal. The relationship between the shown numbers and values of Ψ^2 is as follows: 1 = 0.000 05, 2 = 0.0005, 3 = 0.002, 4 = 0.005, 5 = 0.0125, 6 = 0.025, 7 = 0.05. The dashed lines show nodes.

Table II. Calculated Energies for $M_4(CO)_{12}H_4$ Clusters (eV)

	carbonyls staggered		carbonyls eclipsed	
	edge	face	edge	face
$Fe_4(CO)_{12}H_4$	0.4	[0]	2.9	1.3
$Fe_4(CO)_{12}H_4^{4+}$	1.8	1.4	2.8	[0]

conclusions reached above: Face protonation reduces the barrier to eclipsing (it was 2.0 eV in unprotonated $Fe_4(CO)_{12}^{4-}$) in $Fe_4(CO)_{12}H_4$ and still more so in the electron-deficient cluster with four electrons less. The minimum energy conformation for the latter case is well defined—it is a face-bridging structure with eclipsed carbonyls, in agreement with the known structure of $Re_4(CO)_{12}H_4$.[2]

The equilibrium structure of $M_4(CO)_{12}H_4$, M = Fe, Ru, is less well defined by the calculations. The face-bridging geometry is preferred by 0.4 eV, which does not agree with the observed structures, all edge bridging.[4-6] We are not overly concerned with this disagreement, because the energy difference in our approximate calculation is not large, and also because we know that the related $Co_4Cp_4H_4$ structure has face-bridging hydrogens.[8] Our calculations for a model $Fe_4Cp_4H_4^{4-}$ indeed indicate a large preference of 2.4 eV for face protonation. The detailed rationale for this preference is involved. The energy difference is spread out over a number of orbitals, and is not easy to analyze. However, we can trace part of the extra stabilization of the face sites in the Cp compound over the CO to additional interaction with a second t_2 set. This lies below the framework orbitals shown in Figure 1, and is descended from the t_{2g} set (see **7**) of each fragment. This second t_2 orbital is at higher energy in M_4Cp_4 than $M_4(CO)_{12}$ because there is less back-bonding or stabilization by unfilled terminal ligand orbitals than in the carbonyl case. Though the

Table III. Parameters Used in Extended Hückel Calculations

orbital	H_{ii}, eV	ζ_1	ζ_2	c_1[a]	c_2[a]
Fe 3d	−12.70	5.35	1.8	0.5366	0.6678
4s	−9.17	1.90			
4p	−5.37	1.90			
C 2s	−21.40	1.625			
2p	−11.40	1.625			
O 2s	−32.30	2.275			
2p	−14.80	2.275			
H 1s	−10.0	1.30			

[a] Contraction coefficient used in the double ζ expansion.

calculations were actually carried out for a $Fe_4Cp_4H_4^{4-}$ model, the results should be valid for $M_4Cp_4H_4$, M = Co, Rh, Ir.

Only one entry appears for the edge-bridged hydrides in Table I. Actually we have calculated models for the two structural types found, **3** and **4.** These are essentially indistinguishable in energy, within 0.02 eV of each other.

Our general conclusion is that the parent $Ru_4(CO)_{12}H_4$ system and its substituted derivatives should be characterized by relatively low barriers to movement of hydrogens between edge and face positions. Mobility of hydrogens in $H_4Ru_4(CO)_{12-x}L_x$ (x = 1-4, L = $P(OMe)_3$) has been observed;[4] however, no information is yet available on the pathway traversed by the hydrogen atoms. For the $Ru_4(CO)_{10}H_4$(diphos) case studied by Shapley and co-workers[6] a dynamic process is implicated which involves as waypoints terminal hydrides. These have not as yet been considered in our theoretical studies. The $Re_4(CO)_{12}H_4$ system should have significantly higher barriers to intramolecular tautomerism, which is in accord with experimental findings.[23]

For trihydrides we have studied $Fe_4(CO)_{12}H_3^-$ and $Fe_4Cp_4H_3^{8-}$ as models for the known $Ru_4(CO)_{12}H_3^-$ and $Ni_4Cp_4H_3$ structures.[9-11,24] Four alternative structures were computed for $Fe_4(CO)_{12}H_3^-$, shown in **15–18,** all with

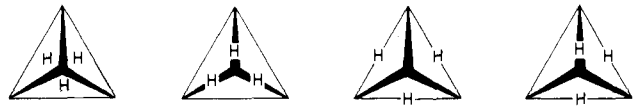

15 **16** **17** **18**

staggered carbonyls. The face-bridged structure **15** comes out 0.3 eV more stable than the three edge-bridged geometries **16–18,** all of which have nearly identical energies. This parallels the results for $Fe_4(CO)_{12}H_4$ mentioned above and is subject to the same reservations. The preference for face bridging in $Fe_4Cp_4H_3^{8-}$ stems from interactions similar to the ones discussed for the four proton system.

The $Ni_4Cp_4H_3$ structure is of special interest because it is so electron rich, exceeding the normal electron count for a tetrahedral cluster by three electrons. In Figure 1 it will be seen that the Ni_4Cp_4 cluster has a low-lying empty t_1 orbital which is split only very slightly in the true reduced symmetry of the cluster. Its contours are shown in Figure 4. By symmetry this orbital has nodes along all C_3 and C_2 axes of the tetrahedron. The orbital is totally unaffected by the addition of three face-bridging hydrogens. For that matter it would be equally unaffected if the hydrogens were edge bridging. As mentioned above, the preference for face bridging over edge bridging is set by other, lower orbitals. The three extra electrons in $Ni_4Cp_4H_3$ populate the (nearly) triply degenerate metal-centered t_1 orbital, explaining the observed paramagnetism of the compound.[9]

Acknowledgment. Support of the work at Cornell came through NSF Grant CHE-76-06099. R.B. acknowledges support from NSF Grants CHE-74-01541 and CHE-77-

00360, and receipt of an NIH Research Career Development Award (CA-00015).

Appendix

The calculations were performed using the extended Hückel method.[25] The H_{ii}'s and orbital exponents for Fe were taken from previous work.[17] The hydrogen H_{ll} was set at -10.0 eV. This places the hydrogens energywise above the valence orbitals of the cluster, giving the H's the character of protons. Calculations with hydrogen H_{ii}'s at -13.6 eV, our normal value, result in a slight change in the magnitude of the calculated energy differences, but do not alter the conclusions reached. The parameters are given in Table III.

The metal–metal distance was kept at 2.54 Å and the cluster geometry tetrahedral. The Fe–C distance in the carbonyl cluster was 1.8 Å, and the distance from the metal to the center of the cyclopentadiene ring in Fe_4Cp_4 was 1.7 Å. The hydrogens were placed 0.86 Å above the cluster face and 1.14 Å from the edge in the face- and edge-protonated systems, respectively.

References and Notes

(1) (a) Cornell University; (b) University of Southern California; (c) University of California; (d) University of Oxford.
(2) (a) R. Saillant, G. Barcelo, and H. D. Kaesz, *J. Am. Chem. Soc.*, **92**, 5739 (1970); (b) R. D. Wilson and R. Bau, *Ibid.*, **98**, 4687 (1976).
(3) H. D. Kaesz, B. Fontal, R. Bau, S. W. Kirtley, and M. R. Churchill, *J. Am. Chem. Soc.*, **91**, 1021 (1969).
(4) (a) H. D. Kaesz, S. A. R. Knox, J. W. Koepke, and R. B. Saillant, *Chem. Commun.*, 477 (1971); S. A. R. Knox and H. D. Kaesz, *J. Am. Chem. Soc.*, **93**, 4594 (1971); (b) B. F. G. Johnson, R. D. Johnston, J. Lewis, B. H. Robinson, and G. Wilkinson, *J. Chem. Soc. A*, 2856 (1968).
(5) R. D. Wilson, S. M. Wu, R. A. Love, and R. Bau, *Inorg. Chem.*, **17**, 1271 (1978).
(6) J. R. Shapley, S. I. Richter, M. R. Churchill, and R. A. Lashewycz, *J. Am. Chem. Soc.*, **99**, 7384 (1977).
(7) J. Müller and H. Dorner, *Angew. Chem.*, **85**, 867 (1973); *Angew. Chem., Int. Ed. Engl.*, **12**, 843 (1973).
(8) G. Huttner and H. Lorenz, *Chem. Ber.*, **108**, 973 (1975).
(9) J. Müller, H. Dorner, G. Huttner, and H. Lorenz, *Angew. Chem.*, **85**, 1117 (1973); *Angew. Chem., Int. Ed. Engl.*, **12**, 1005 (1973).
(10) G. Huttner and H. Lorenz, *Chem. Ber.*, **107**, 996 (1974).
(11) T. F. Koetzle, R. K. McMullan, R. Bau, D. W. Hart, R. G. Teller, D. L. Tipton, and R. D. Wilson, *Adv. Chem. Ser.*, in press.
(12) K. Wade, *Chem. Commun.*, 792 (1971); *Inorg. Nucl. Chem. Lett.*, **8**, 559, 563 (1972); "Electron Deficient Compounds", Nelson, London, 1971; *Adv. Inorg. Chem. Radiochem.*, **18**, 1 (1976).
(13) D. M. P. Mingos, *Nature (London), Phys. Sci.*, **238**, 99 (1972); R. Mason and D. M. P. Mingos, *MTP Int. Rev. Sci.: Phys. Sci., Ser. Two*, 11, 121 (1975); D. M. P. Mingos and M. I. Forsyth, *J. Chem. Soc., Dalton Trans.*, 610 (1977).
(14) Trinh-Toan, W. P. Fehlhammer, and L. F. Dahl, *J. Am. Chem. Soc.*, **94**, 3389 (1972); A. S. Foust, M. S. Foster, and L. F. Dahl, *ibid.*, **91**, 5633 (1969).
(15) J. W. Lauher, to be published.
(16) M. Elian, M. M.-L. Chen, D. M. P. Mingos, and R. Hoffmann, *Inorg. Chem.*, **15**, 1148 (1976). See also ref 12–15 and J. E. Ellis, *J. Chem. Educ.*, **53**, 2 (1976).
(17) T. A. Albright, P. Hofmann, and R. Hoffmann, *J. Am. Chem. Soc.*, **99**, 7546 (1977).
(18) M. Elian and R. Hoffmann, *Inorg. Chem.*, **14**, 1058 (1975).
(19) See R. Hoffmann and W. N. Lipscomb, *J. Chem. Phys.*, **36**, 2179 (1962), for a discussion of this problem in the boron hydrides.
(20) C. Glidewell, *Inorg. Nucl. Chem. Lett.*, 11, 761 (1975).
(21) R. B. King, *Inorg. Chem.*, **16**, 1822 (1977); R. B. King and D. H. Rouvray, *J. Am. Chem. Soc.*, **99**, 7834 (1977).
(22) S. F. A. Kettle, *Theor. Chim. Acta*, **4**, 150 (1966); S. F. A. Kettle and V. Tomlinson, *Ibid.*, **14**, 175 (1969); *J. Chem. Soc. A*, 2002, 2007 (1969); S. F. A. Kettle and D. J. Reynolds, *Theor. Chim. Acta*, **22**, 239 (1971).
(23) M. A. Andrews and H. D. Kaesz, to be published.
(24) J. W. Koepke, J. R. Johnson, S. A. R. Knox, and H. D. Kaesz, *J. Am. Chem. Soc.*, **97**, 3947 (1975).
(25) R. Hoffmann, *J. Chem. Phys.*, **39**, 1397 (1963); R. Hoffmann and W. N. Lipscomb, *ibid.*, **36**, 2179, 3489 (1962); **37**, 2872 (1962).

The Band Structure of the Tetracyanoplatinate Chain

Myung-Hwan Whangbo and Roald Hoffmann*

Contribution from the Department of Chemistry, Cornell University, Ithaca, New York 14853. *Received September 6, 1977*

Abstract: The band structure of the tetracyanoplatinate chain is examined in the tight-binding approximation based on the extended Hückel method. The unit cell contains a staggered $[Pt(CN)_4]_2^{4-}$, and the calculation is repeated at various Pt–Pt separations. The free electron nature of the bands is probed by computing effective masses. From the band structure and the density of states one derives an expression for the total energy per unit cell as a function of partial oxidation of the polymer. The equilibrium Pt–Pt separation so estimated decreases to less than 3 Å for a loss of 0.3 electron per platinum, in reasonable agreement with structural studies. Details of the band structure are supported by explicit and simple molecular orbital arguments.

A class of partially oxidized one-dimensional conducting salts of tetracyanoplatinate, $Pt(CN)_4^{2-}$, has been one of the most extensively studied low-dimensional conducting materials.[1] The crystal structures of these compounds contain the planar platinum complex, $Pt(CN)_4^{2-}$, stacked together to form parallel linear or nearly linear chains of Pt atoms.[2] Structural and chemical observations on these compounds reveal that the Pt atoms are all equivalent, and thus they are in a single partial oxidation state, and that the Pt–Pt distance (r_{Pt-Pt}) becomes shorter with increase in the partial oxidation number of Pt.[2] In a band picture the fractional oxidation state of Pt corresponds to a partially filled band. Experiments on $K_2[Pt(CN)_4]Br_{0.3}\cdot 3H_2O$ (KCP) indicate that except for the Peierls instability the conduction electrons in KCP behave as nearly free electrons along the Pt chain.[3] Further, this free electron character persists among the analogues of KCP despite a large variation of r_{Pt-Pt} in these compounds.

Calculations of the band structure of the $Pt(CN)_4^{2-}$ chain reported so far have considered in general only a linear chain of Pt atoms.[4,5] A three-band model (i.e., inclusion of $5d_{z^2}$, 6s and $6p_z$ of Pt, where z refers to the Pt-chain axis) was found inadequate for the description of the electronic structure of KCP.[4a] Under the assumption that the CN^- ligands force the Pt atom to adopt a wave vector independent s–d hybridization, a two-band model (i.e., inclusion of s–d hybrid and p_z orbitals) produces a free-electron-like band.[4a] An important recent calculation by Bullett considers the full $Pt(CN)_4^{2-}$ chain.[5b]

In the present work the band structure of the $Pt(CN)_4^{2-}$ chain was examined within the tight-binding scheme[6] based upon the extended Hückel method.[7] Our calculations included all the valence atomic orbitals of the Pt, C, and N atoms of a unit cell in the $Pt(CN)_4^{2-}$ chain. Questions of theoretical importance in the electronic structure of the $Pt(CN)_4^{2-}$ chain are (a) the free-electron behavior of the conduction electrons

0002-7863/78/1500-6093$01.00/0